Reaction-diffusion waves in hydro-mechanically coupled porous solids

Qingpei Sun[1], Manman Hu[1], Christoph Schrank[2], Klaus Regenauer-Lieb[3]

[1]Department of Civil Engineering, The University of Hong Kong, Hong Kong [2]School of Earth and Atmospheric Sciences, Queensland University of Technology, Brisbane, QLD, 4001, Australia [3]School of Minerals and Energy Resources Engineering, UNSW, Sydney, NSW 2052 Australia

Key Points:

- A new class of nonlocal reaction-diffusion equations models Earth instabilities
- Stationary and travelling dissipative waves are predicted
- Turing, Hopf and quasi-soliton waves create barcode-like fault damage zones

Corresponding author: Manman Hu, `mmhu@hku.hk`

Abstract

Here, we extend the Fisher-Kolmogorov-Petrovsky-Piskunov equation to capture the interplay of multiscale and multiphysics coupled processes. We use a minimum of two coupled reaction-diffusion equations with additional nonlocal terms that describe the coupling between scales through mutual cross-diffusivities. This system of equations incorporates the physics of interaction of thermo-hydro-chemo-mechanical processes and can be used to understand a variety of localisation phenomena in nature. Applying bifurcation theory to the system of equations suggests that geological patterns can be interpreted as physical representation of three classes of well-known instabilities: Turing instability, Hopf bifurcation, and a chaotic regime of complex soliton-like waves. For specific parameters, the proposed system of equations predicts all three classes of instabilities encountered in nature. The third class appears for small fluid release reactions rates as a slow quasi-soliton wave for which our parametric diagram shows possible transition into the Hopf- or Turing-style instability upon dynamic evolution of coefficients.

Plain Language Summary

Regular and irregular patterns of deformation bands and fractures are ubiquitous in nature. In this paper, we decipher the patterns in terms of coefficients of a simple set of reaction-diffusion equations that can, for a given set of material parameters, describe a transition from regular to logarithmically decaying patterns and chaotic instabilities. The set of equations has previously been used to explain phenomena in complex chemistry and pattern formation in epidemiology, but without the multiscale and multiphysics consideration presented here. This work introduces the mathematical formulation and analysis, and quantitative applications to geological observation will follow.

1 Introduction

Travelling-wave solutions of reaction-diffusion systems are encountered in many fields, e.g. in chemistry, epidemiology, biology, medicine, and physics. They were first identified in chemistry by R. Luther in 1906 and demonstrated in an experiment where oxalic acid mixed with potassium permanganate led to a wave propagation of the reaction made visible by an oscillatory front of decolorization of the mixture. An English translation of the transcript of the original lecture has been published much later (Luther, 1987). Subsequently, the same fundamental partial differential reaction-diffusion equation was shown by R.A. Fisher to explain wave-like propagation of mutant genes (Fisher, 1937), which is widely used in epidemiology for modeling the spread of viruses as well as in many other field of biology (Volpert & Petrovskii, 2009). The equation is now better known as the Fisher-Kolmogorov-Petrovsky-Piskunov (FKPP) equation (Kolmogorov et al., 1937), recognizing the important early work (Adomian, 1995).

Although the basic mathematical equation is agnostic of the application, and the phenomenon is now well established in the above named disciplines, it has found little application in the Earth Science field so far, where reaction-diffusion problems are common. Pioneering work was presented in the 1990's (Dewers & Ortoleva, 1990; Ortoleva, 1993, 1994). Not much progress has been made on further development of geophysical applications to the slow travelling-wave solution. Broader community interest was mainly met for the special case of the stationary solution of the system of equations (Ball, 2012). The main problem in the application to Earth Sciences is perhaps twofold. The first problem is that patterns in nature are mostly observed as frozen in features of the dynamic solution and it is difficult to discern from geological observations, whether the rhythmic features are frozen-in patterns of an oscillating reaction-diffusion equation propagating in time, or whether they are caused by a standing wave solution fixed in space (L'Heureux, 2013). The second problem is that the original FKPP equation does not replicate the rich field of observations encountered in nature.

For geological applications, a generalized power-law reactive source term therefore has been proposed as an extension to the FKPP equation (Vardoulakis & Sulem, 1995). Using the simple case of a time-independent reaction-diffusion equation with a power-law reactive source term and integer-valued exponents, standing solitary wave Korteweg-De Vries (KdV)-type solutions were obtained analytically (Regenauer-Lieb et al., 2013; Veveakis & Regenauer-Lieb, 2015). The inclusion of the power-law source term unfortunately leads to an infinite amplitude KdV-type solitary wave. Several attempts have been made to overcome this shortcoming with the aim to provide an appropriate application for modelling compaction bands in porous (or multiphase) geomaterials. Among them, the most impressive one is a specific solution proposed by an additional reaction source term buffering the instabilities for carefully chosen cases (Alevizos et al., 2017). While the proposed approaches manage to achieve a solution to the ill-posed problem of lacking an internal material length for some cases, a generalized approach is in absence.

Here, we develop a theory that has the potential to solve the problem directly for all cases by using an approach that is based on internal length scales stemming from the physics of the feedbacks of multiple processes operating across multiple characteristic scales. We introduce the lacking internal material length scale through an integration of non-local diffusion and reaction coefficients originating from lower-scale processes. In a simple formulation, the feedbacks can be captured mathematically by the interaction between at least two reaction-diffusion equations coupled through two sufficiently large cross-diffusion coefficients between interweaved dynamic systems, e.g., a saturated porous medium in the post-yield regime (Hu et al., 2020).

The system of equations has been generalized to describe multiphysics couplings between multiple scales (Regenauer-Lieb et al., 2021). In such a formulation, the cross-diffusion coefficients are derived through volume integration of diffusion processes that are spatially connected to interactions at the lower scale and therefore also called non-local diffusion processes. In this sense, the diffusion of a given concentration of species does not only depend on its position in space and its gradient, but also on the nonlocal effect of the values of concentrations around it and the convolution of the concentration with the probability distribution to jump from one location to another (Amdreo-Valle et al., 2010). Such nonlocal diffusion processes have recently attracted much attention from the mathematics community as the FKPP-equation was found to display unexpected wave front accelerations due to the nonlocal terms, as first observed in the invasion of cane toads in Australia (Bouin et al., 2017).

As an innovation in this paper, we also consider nonlocal reactions where the non-locality arises from modeling the behavior of one phase interacting with another in its immediate environment and vice versa, concurrently - lending itself to a dynamical system approach that captures the multiphysics involved in a tightly coupled fashion. The beauty of this new class of nonlocal approaches lies in the fact that it naturally allows process coupling across spatial and temporal scales where runaway reactions can be buffered via infinite-speed propagation of such perturbations through the nonlocal diffusion process (Amdreo-Valle et al., 2010). In this letter, we perform a linear stability analysis of the newly proposed system of equations, revealing three fundamentally different types of instabilities.

2 Korteweg-De Vries-type standing-wave limit

The dynamic equation for the momentum balance of the solid skeleton in a hydro-poromechanic nonlinear visco-plastic medium is expressed in the Perzyna overstress (Duszek-Perzyna & Perzyna, 1996) formulation (describing the viscous material behaviour post yield) as a FKPP-type reaction-diffusion equation:

$$\frac{\partial \bar{p}_s}{\partial t} = D_M \frac{\partial^2 \bar{p}_s}{\partial x^2} + R_1, \tag{1}$$

where in the above 1-D formulation $\bar{p}_s$ denotes the Perzyna overpressure for the solid skeleton and R_1 a nonlinear reactive source pressure term.

Under the standing-wave assumption, this travelling-wave equation becomes a static mechanical viscous overpressure reaction-diffusion equation:

$$D_M \frac{\partial^2 \bar{p}_s}{\partial x^2} + R_1 = 0. \tag{2}$$

The coupled dynamic fluid pressure system can be described by a similar wave equation:

$$\frac{\partial p_f}{\partial t} = D_H \frac{\partial^2 p_f}{\partial x^2} + R_2, \tag{3}$$

which for the static case with a zero source term R_2 becomes the Darcy equation:

$$D_H \frac{\partial^2 p_f}{\partial x^2} = 0. \tag{4}$$

We introduce a dimensionless form

$$\tilde{p}_s = \frac{\bar{p}_s}{p'_{ref}} \; , \; \tilde{x} = \frac{x}{l_0}, \lambda = \frac{D_M}{D_H}, \tag{5}$$

where p'_{ref} and l_0 are reference pressure and reference length, respectively. Assuming a power-law reactive pressure source term with a power-law exponent m, the coupled system of equations (2) and (4) becomes a Korteweg-De Vries-type standing wave equation:

$$\frac{\partial^2 \tilde{p}_s}{\partial \tilde{x}^2} - \lambda \tilde{p}_s^m = 0. \tag{6}$$

Analytical solutions for the practical application to compaction bands with $m = 3$ have been suggested (Regenauer-Lieb et al., 2013; Veveakis & Regenauer-Lieb, 2015), which feature, for a critical ratio of solid/fluid self-diffusivities $\lambda > 12.7$, periodic standing waves with infinite-amplitude singularities of the non-dimensional overpressure.

3 Cross-diffusion equations in geomaterials

The system of equations can be regularized by extending equations (1) and (3) through nonlocal cross-coupling diffusivities between the two dynamic systems considering the unique structure of porous media (Hu et al., 2020). Such cross-couplings are well known in chemistry as cross-diffusion (Vanag & Epstein, 2009) between chemically reactive constituents. In our case, cross-diffusion arises as interfacial characteristics (Hu et al., 2020) and regularizes the feedbacks between the dynamic evolution of the fluid and solid pressure. The equations for a fully saturated porous medium post yield can be expressed as:

$$\frac{\partial \bar{p}_s}{\partial t} = D_M \frac{\partial^2 \bar{p}_s}{\partial x^2} + d_H \frac{\partial^2 p_f}{\partial x^2} + R_1, \tag{7}$$

$$\frac{\partial p_f}{\partial t} = d_M \frac{\partial^2 \bar{p}_s}{\partial x^2} + D_H \frac{\partial^2 p_f}{\partial x^2} + R_2, \tag{8}$$

where R_1 and R_2 are the reaction terms in the governing equations for solid and fluid pressure, respectively. For completeness, we extend the formulation of the crossover diffusion problem proposed earlier (Hu et al., 2020) by nonlocal reaction terms. This allows us to explore a more general solution space.

For expanding the reaction term R_2 in Eq.(8), we need to consider the feedback between solid and fluid pressure reactions. The reaction term R_2 incorporates cross-scale coupling to gradients of the pressure in the solid matrix p_s in the surrounding pore space, which exerts a "nonlocal" effect on the fluid pressure p_f inside the pore. For the local source term, we assume a simple linear process for the fluid phase, which can be water production/depletion due to dehydration/rehydration of minerals. Thus, to take into account the above two factors, we assume that the reaction term R_2 follows a linear function of the fluid pressure and solid overstress, i.e. $R_2 = a_{21}\bar{p}_s + a_{22}p_f$, where a_{21} and a_{22} are the corresponding coefficients.

Likewise, the reaction term R_1 in Eq.(7) is translated into a nonlocal reaction formulation as we expand the power-law assumption in (Veveakis & Regenauer-Lieb, 2015) by higher order terms of $\bar{p}_s$ to describe the viscoplastic behaviour of the solid skeleton. The feedback to the fluid pressure p_f is, however, assumed to be linear, for simplicity. The generalized reaction term in Eq.(7) is now written in a non-linear form of $R_1 = a_{11}\bar{p}_s + a_{12}p_f + a_{13}\bar{p}_s^2 + a_{14}\bar{p}_s^3$. Note that all the coefficients in the reaction terms would also evolve according to the in-situ chemo-hydro-mechanical conditions, but here we just give the generalized form and regard them as constants to facilitate the analysis.

By introducing the dimensionless parameters $\tilde{t} = \dot{\varepsilon}_0 t$, $\tilde{p}_f = \bar{p}_f / p'_{ref}$, where $\dot{\varepsilon}_0$ denotes the reference strain rate, together with the previously defined $\tilde{p}_s = \frac{\bar{p}_s}{p'_{ref}}$, $\tilde{x} = \frac{x}{l_0}$, we arrive at the normalized cross-diffusion equations with normalized reaction terms $\tilde{R}_1$ and $\tilde{R}_2$ expressed as

$$\frac{\partial \tilde{p}_s}{\partial \tilde{t}} = \tilde{D}_M \frac{\partial^2 \tilde{p}_s}{\partial \tilde{x}^2} + \tilde{d}_H \frac{\partial^2 \tilde{p}_f}{\partial \tilde{x}^2} + \tilde{a}_{11}\tilde{p}_s + \tilde{a}_{12}\tilde{p}_f + \tilde{a}_{13}\tilde{p}_s^2 + \tilde{a}_{14}\tilde{p}_s^3, \tag{9}$$

$$\frac{\partial \tilde{p}_f}{\partial \tilde{t}} = \tilde{d}_M \frac{\partial^2 \tilde{p}_s}{\partial \tilde{x}^2} + \tilde{D}_H \frac{\partial^2 \tilde{p}_f}{\partial \tilde{x}^2} + \tilde{a}_{21}\tilde{p}_s + \tilde{a}_{22}\tilde{p}_f, \tag{10}$$

where $\tilde{D}_M = \frac{D_M}{l_0^2 \dot{\varepsilon}_0}$, $\tilde{d}_H = \frac{d_H}{l_0^2 \dot{\varepsilon}_0}$, $\tilde{a}_{11} = \frac{a_{11}}{\dot{\varepsilon}_0}$, $\tilde{a}_{12} = \frac{a_{12}}{\dot{\varepsilon}_0}$, $\tilde{a}_{13} = \frac{a_{12}p'_{ref}}{\dot{\varepsilon}_0}$, $\tilde{a}_{14} = \frac{a_{12}p'_{ref}{}^2}{\dot{\varepsilon}_0}$, $\tilde{d}_M = \frac{d_M}{l_0^2 \dot{\varepsilon}_0}$, $\tilde{D}_H = \frac{D_H}{l_0^2 \dot{\varepsilon}_0}$, $\tilde{a}_{21} = \frac{a_{21}}{\dot{\varepsilon}_0}$, $\tilde{a}_{22} = \frac{a_{22}}{\dot{\varepsilon}_0}$.

In this paper, we describe only two coupled nonlocal reaction-diffusion processes while it is straightforward to extend the approach into a higher degree of coupling such as an interaction with a thermal nonlocal reaction diffusion equation. Without loss of generality, we also limit the higher-order expansion to the order 3 for numerical analysis to capture the essential features of the formulation. In our investigation, an order 3 was the minimum requirement to obtain the full spectrum of solutions including excitation waves. The development of a concise formulation for extension to higher degrees of coupling is never a trivial task considering the complexity associated with new spatial and temporal scales introduced into the system, and is hence out of the scope of this letter. A simplified meso-scale formalism is proposed in (Regenauer-Lieb et al., 2021) by adding additional cross- and self-diffusion coefficients to the system of equations via the fully populated true diffusion matrix.

3.1 System constraints and system behaviour

In what follows, the behaviour of a system of saturated porous material described by Eq.(9) and Eq.(10) for $\tilde{p}_s : \Omega \to \mathcal{R}^1$ and $\tilde{p}_f : \Omega \to \mathcal{R}^1$, respectively, will be investigated. We use a classical formulation for modelling wave-propagation problems. Non-flux boundary conditions are assumed: $\mathbf{n} \cdot \nabla \tilde{p}_s = 0$ and $\mathbf{n} \cdot \nabla \tilde{p}_f = 0$ for $x \in \partial\Omega$. Here, $\Omega \subset \mathcal{R}^n$ is a smooth bounded domain with outer unit normal $\mathbf{n}$ and total volume $\mid \Omega \mid$. The initial condition is assumed as $\tilde{p}_s(x, 0) = \tilde{p}_f(x, 0) = 0$ for $x \in \Omega$, for simplicity.

In terms of the Perzyna overstress model used in this formulation, the system size is considered to correspond to the region where the overstress has been reached due to loading from the far field. The non-flux boundary conditions then correspond to the elastic-plastic boundary. In what follows, we arbitrarily choose the left boundary as the one where the system receives a perturbation from the outside which may lead to material failure within or at the boundaries of the system.

While the addition of a cross-diffusion term allows a fast response to the coupling of the two dynamical equations, thus regulating the coupled system by the new cross-diffusivities, the equations become no longer tractable in analytical form. The coupling terms may also give rise to new instabilities, for which the linear stability analysis (see Supporting Information) provides a robust derivation. With sufficiently large perturbation applied on the left boundary of the domain, three different types of instabilities are encountered: (1) Turing instabilities, (2) Hopf-bifurcations, and (3) cross-diffusional waves. The corresponding systems are investigated numerically in the following subsections. Selections of parameters are based on the linear stability analysis presented in the Supporting Information.

3.2 Turing bifurcations

When the system undergoes Turing bifurcations, standing waves are generated, leading to space-periodic patterns. Turing bifurcations require the system to be stable when diffusion is not considered, and an unstable saddle comes into effect when the control parameters vary (see Supporting Information). In our formulation, the phase space is spanned by the two main variables $\tilde{p}_s$ and $\tilde{p}_f$, and the main control variables for these are $\tilde{a}_{11}$ snd $\tilde{a}_{22}$, scaling the sign and magnitude of the solid and fluid pressure reactive source terms, respectively. A saddle point in the $\tilde{p}_s$ - $\tilde{p}_f$ phase space is defined as a critical point where the phase switches from a stable manifold to an unstable manifold. In other words: (I) a stable manifold is achieved via $Re(s_k) < 0$, i.e. the real part of s_k being negative, when the wavenumber $k = 0$; (II) an unstable manifold exists with the variation of wavenumber k, if a real positive number (no imaginary part) exists for s_k, which corresponds to the growth rate of the perturbation. To satisfy the above requirements, a sufficient condition for the onset of Turing instabilities is summarized as follows:

(a) $\text{tr}_0 = \tilde{a}_{11} + \tilde{a}_{22} < 0$, where tr_0 denotes the value of tr_k for wavenumber $k = 0$.

(b) $\Delta_0 = \tilde{a}_{11}\tilde{a}_{22} - \tilde{a}_{12}\tilde{a}_{21} > 0$, where Δ_0 denotes the value of Δ_k for wavenumber $k = 0$.

Here, tr_k and Δ_k are coefficients in the characteristic polynomial of s_k as defined in the Supporting Information.

(c) At the critical wavenumber k_c,

$$k_c^2 = \frac{\tilde{a}_{11}\tilde{D}_H + \tilde{a}_{22}\tilde{D}_M - \tilde{a}_{21}\tilde{d}_H - \tilde{a}_{12}\tilde{d}_M}{2(\tilde{D}_M\tilde{D}_H - \tilde{d}_M\tilde{d}_H)},$$

$$\Delta_{k_c} = \Delta_0 - \frac{(\tilde{a}_{11}\tilde{D}_H + \tilde{a}_{22}\tilde{D}_M - \tilde{a}_{21}\tilde{d}_H - \tilde{a}_{12}\tilde{d}_M)^2}{4(\tilde{D}_M\tilde{D}_H - \tilde{d}_M\tilde{d}_H)} < 0.$$

Since the current cross-diffusion formulation is essentially a mass balance based approach, it is expected that the two self-diffusion coefficients $\tilde{D}_M$ and $\tilde{D}_H$ are positive and that the two cross-diffusion coefficients $\tilde{d}_M$ and $\tilde{d}_H$ are of opposite sign. Hence, $(\tilde{D}_M\tilde{D}_H - \tilde{d}_M\tilde{d}_H) > 0$ is naturally satisfied, i.e. Δ_k at the critical wavenumber corresponds to a local minimum. This criterion combines the self- and cross-diffusion coefficients and extends the original formulation for Turing instabilities (Regenauer-Lieb et al., 2013; Veveakis & Regenauer-Lieb, 2015).

It is worth noting that the characteristic Turing wavelength is an intrinsic characteristic for the reaction-diffusion equation. It is $\lambda = 2\pi/k_c$, which shows that the wave length is determined by the material coefficients and the system properties comprising the diffusivities and the size of the system (plastic zone) considered (Regenauer-Lieb et al., 2013). This implies that if the size of the plastic zone is known, the diffusive material properties can directly be derived from the observation of the localisation pattern, e.g., the spacing of fractures or deformation bands (Elphick et al., 2021; Hu et al., 2020), since the diffusion properties also control the spacing of the pattern.

To illustrate the Turing bifurcation solution, we plot numerical results obtained with the Finite Difference Method (FDM) in Fig. (1a) and Fig. (1b).

The Turing-style instabilities lead to an equally spaced segmentation of the plastic zone with a distinct striped pattern of localisation (Fig. 1b). Upon continued deformation, the system size and the diffusivities change because inelastic strain localisation modifies the material properties, strain, and the local state of stress. For example in the case of compaction of the plastic zone, the entire zone shrinks continuously, accommodated by discrete Turing-patterned compaction bands. Compaction also changes the diffusivities because permeability is commonly reduced due to inelastic porosity loss through, e.g., grain crushing in the bands (Elphick et al., 2021). Finally, low-porosity compaction bands are also expected to cause local elastic stress amplification, facilitating further strain localisation (Elphick et al., 2021). These effects are not considered in our current calculation. However, for cases where only small deformations are encountered, we expect preservation of Turing-style deformation since the Turing standing wave is essentially a stationary solution.

3.3 Hopf bifurcations

When the system undergoes Hopf bifurcations, travelling waves are generated, and temporally periodic (oscillation) patterns can be found (see Fig. 2). The Hopf bifurcation changes a stable focus ($\mathrm{Re}(s_k) < 0$) into an unstable one ($\mathrm{Re}(s_k) > 0$) with the change of control parameters. This requires the existence of certain complex number s_k with the real part (i.e., $\frac{1}{2}\mathrm{tr}_k$) no less than zero when the wavenumber k varies. Given that the maximum value of tr_k is always obtained when $k = 0$, the above requirement for Hopf instability can be translated to $\mathrm{tr}_0 = \tilde{a}_{11} + \tilde{a}_{22} \geq 0$, $\mathrm{tr}_0{}^2 - 4\Delta_0 = (\tilde{a}_{11} + \tilde{a}_{22})^2 - 4(\tilde{a}_{11}\tilde{a}_{22} - \tilde{a}_{12}\tilde{a}_{21}) < 0$.

The characteristics of Hopf bifurcations are illustrated with numerical solutions obtained with FDM in Fig. (1c) and Fig. (1d). The periodic solutions are similar to Turing bifurcations, replacing a singular frequency spectrum with an exponentially decaying frequency spectrum (Fig. 1c). The oscillation frequency f of the Hopf bifurcation is an intrinsic material property of the reaction-diffusion equation and is defined by $f = 1/T = \sqrt{\tilde{a}_{11}\tilde{a}_{22} - \tilde{a}_{12}\tilde{a}_{21}}/2\pi$. Inversion of material properties from temporal observation thus appears to be possible.

In our example calculation shown in Fig. (1c) and Fig. (1d), the frequency spectrum has distinct gaps between the longest waves and the shortest wavelength at the zero-flux (reflecting) opposite boundary of the plastic zone. As the waves are dissipative, they act like damage waves that continuously change the mechanical properties of the medium they traverse. An important observation is that the travelling Hopf wave does not reflect from the system boundary but dumps its energy into the boundary.

3.4 Cross-diffusion waves for the excitable system

With the variation of parameters in reaction terms $\tilde{R}_1$ and $\tilde{R}_2$, we encounter a slow reaction case where the coefficients in $\tilde{R}_2$ are much smaller than those in $\tilde{R}_1$. In this case, the whole system would become excitable, and soliton-like behaviours can be observed.

This situation differs significantly from the above solutions. Upon initiation, the wave does not contain information of the system size but constitutes a pure material instability, carrying only information on the material defining the cross-diffusion matrix (Tsyganov et al., 2007). Upon reflection on the opposite boundaries of the plastic zone, the wave can, however, 'sense' the system size and alter its behaviour accordingly. A special characteristic of a quasi-soliton is that it does not depend on initial conditions but its propagation velocity is a material constant which does not alter after reflection (Tsyganov et al., 2007).

Fig. (1e) and Fig. (1f) illustrate the behaviour of quasi-soliton travelling waves in an excitable system prior to collision or reflection on boundaries with numerical simulations. Our results show that the frequency content changes after interaction with boundaries. Fig. (1e) shows the frequency spectrum after first collision with the boundary where the wave picks up its first information of the system size. Prior to collision with the right boundary, the wave is unaffected by the system size, which is an important difference to the Turing and Hopf style instability. The speed of the dominant wave group of the quasisoliton is a material property and independent of initial conditions (Tsyganov et al., 2007). An important aspect is the maximum amplitude at zero frequency, or 'infinite' wavelength, which suggests that relativistic considerations need to be introduced for high wave speeds which are not expected to be encountered in geological applications. We show in Fig (1e) a frequency plot after interaction with the opposite boundary which moves the zero frequency maximum to a low frequency maximum.

The frequency spectrum and the behaviour of these waves are complex. Our numerical results show that the cross-diffusion waves can behave like solitons, i.e., they can penetrate through each other or reflect from boundaries. However, there are a number of significant differences (Tsyganov & Biktashev, 2014): (1) their amplitude and speed depend entirely on material parameters whereas those of true solitons depend on initial conditions, (2) true solitons do not change after interpenetration or reflection from boundaries while quasi-soliton waves change frequency spectrum and amplitudes after interaction, and (3) their peculiar behaviour upon collision/reflection classifies them as quasi-solitons encountered in particle physics as they behave like unstable particles (Lioubashevski et al., 1996) and in the extreme case can lead to catastrophic instabilities (Eberhard et al., 2017) sampling wave energy over multiple length scales to release it in a rogue wave.

4 Discussion

Excitation-wave theory has progressed greatly in Russia following the seminal paper by Kolmogorov et al. (1937) on the FKPP equation. Excitation waves are self-excited waves designated as a new fundamental class of waves encountered in all reaction-diffusion systems in physics, biology, and chemistry (Vasil'ev, 1979). Although significant progress has been made in biology, epidemiology, medicine and other fields, the progress in Earth Sciences has been limited to only a few contributions. The closest bridge to geomaterials is in material science and particular metal deformation processes which can be used to better understand basic phenomena. Metals provide simpler crystallographic structures and less complex compositions than rock-forming minerals. An excellent review of the application of self-excitation theory crossing material and geoscience disciplines is available (Makarov & Peryshkin, 2017). The review elaborates on the key hypothesis that slow self-excitation waves propagate at different scales in fault damage zones. They are postulated to be a common physical phenomenon in geomaterials. They have, however, not yet been detected by geophysical methods as they require new low frequency sensors. Empirical comparisons of the excitation wave phenomenon with processes in fault zones are described in (Kuz'min, 2012).

To discuss the geoscientific implications of our newly proposed nonlocal reaction-diffusion equation, we map the three fundamental classes of instabilities - Turing-, Hopf-

, and excitation waves - in the parametric space $\tilde{a}_{11}-\tilde{a}_{22}$ (Fig. 3). The control parameters $\tilde{a}_{11}$ and $\tilde{a}_{22}$ represent the first-order coefficients of the solid and fluid pressure reaction rates $\tilde{R}_1$ and $\tilde{R}_2$. Although we need an order 3 expansion for the mechanical reaction term to obtain excitation waves, these first-order terms fully control the onset of excitation wave instabilities. We find that the appearance of the self-excitation wave corresponds to a narrow domain (highlighted polygon in Fig. 3) where $\tilde{a}_{11}$ is negative and the magnitude of the coefficient for fluid pressure rate $\tilde{a}_{22}$ is small. Interestingly, excitation waves are even possible for very small negative $\tilde{a}_{11}$, corresponding to very small values of solid overstress rate (low tectonic loads).

The fact that in our stability analysis excitation waves are expected for such low values in mechanical reaction rates $\tilde{R}_1$ coupled with low reaction rate $\tilde{R}_2$ (slow production of fluid pressure source from chemical reactions) implies that such excitation waves are common features. An example for such low fluid pressure source terms is the dissolution-precipitation reaction during diagenesis or metamorphic breakdown which occurs on long time scales. These reactions are therefore expected to trigger slow excitation waves which may be interpreted geologically as the first step in a long road to failure.

The modification of an originally homogeneous material into a structured one may, under continued geodynamic loading, lead to further amplification of the applied stress, resulting in the activation of high-stress micro-deformation processes such as crystal-plastic dislocation creep. Zaiser and Hähner (1997) describe a range of processes in this dislocation regime which can lead to an oscillatory response. These oscillatory phenomena encountered in metals and alkali halides have been identified as an excitable wave phenomenon (Zuev & Barannikova, 2010) based on the particle-like discrete foundation of their slip systems.

Similar to the self-excitation waves, the Turing instability occupies only a narrow domain of parameters while the Hopf instability covers the largest section of the mapped space (Fig. 3). One would therefore expect Hopf bifurcations to be most common in nature because they cover the largest parameter space. Hopf waves occur for either a positive $\tilde{a}_{11}$ or a sufficiently large $\tilde{a}_{22}$ in the case of a negative $\tilde{a}_{11}$. Hopf and Turing bifurcations have been applied to explain the rhythmic layering observed in many geological/chemical systems as found in experiments where oscillatory reactions occur in solid solutions grown from aqueous solutions (L'Heureux, 2013).

Hopf- and Turing-style instabilities in geomaterials have first been described by Dewers and Ortoleva (1990). The authors formulate a mathematical model for interaction between chemical and mechanical thermodynamic forces and fluxes that appear in randomly varying mixtures of mechanically strong and weak reacting minerals in the presence of an applied stress field. Stress concentrations in the stronger phase were described to increase the chemical potential and lead to transport down chemical potential gradients into regions initially depleted in the strong phase. This positive feedback between chemical and mechanical thermodynamic forces leads to chemo-mechanical oscillations where textural variations become amplified. In their introduction, Dewers and Ortoleva (1990) describe many observations of metamorphic patterns, resulting from a change in the structure of an initially random material into a strongly layered medium.

In our analysis, we found that Hopf waves do not reflect from boundaries but dump their energy into them. This property could become important as a potential mechanism for pre-seismic slip on a future major fault. While in this simulation the Hopf waves focus cumulative damage on the opposite boundary, in a more realistic geological scenario damage accumulation can occur on pre-existing faults or fractures, which can act as internal elastic-plastic system boundaries embedded in the large-scale plastic zone. The Hopf bifurcation is therefore here interpreted to prepare a given internal structure for failure. In this sense, we may speculate that, in terms of geological interpretation, Hopf

bifurcations could be a mechanism for generating distributed fault damage zones as defined in Table 1 in Peacock et al. (2017).

For the Hopf bifurcation, our simulations show two regimes with an irregular pattern: a transient regime prior to the wave reaching the opposite boundary with exponentially decaying frequency-amplitude relationships, and a post-boundary interaction regime with a stable orbit (Fig. 2), also with an exponential frequency-magnitude relationship (Fig. 1c). Similar patterns have been reported in the geological literature (Elphick et al., 2021). For the application of the approach to geology, L'Heureux (2013) emphasizes the caveat that it is impossible to differentiate between the dynamic or stable-orbit type of solution. The time sequence of the pattern development requires careful microstructural and field geological analysis which is beyond the scope of this contribution.

The quasi-soliton (cross-diffusion) wave solution has the interesting property that the velocity of the wave is a material property and not affected by initial conditions. Once the wave is triggered by perturbations, it continues and sustains itself (at perpetuity if the coefficients do not change) as a self excitation wave. The quasi-soliton (auto)wave is argued here to be the most often encountered in nature as chemical fluid-release reactions are often very slow, thus favouring the nucleation of cross-diffusion waves. It may be seen to prepare the material for Hopf- or Turing bifurcations or directly lead to catastrophic instabilities.

The propagating cross-diffusion waves lead to continuous material damage, which in turn changes the material parameters over time, accelerating the reaction rates and pushing the deforming system out of the stability diagram for quasi-soliton waves. These waves are dissipative waves that travel through the material leaving a different structure in their wake. They may be seen as the dynamic solution of a continuum damage mechanics approach from a thermodynamic perspective. They do not generally form stable localisation bands as they have finite group velocity and can be reflected from internal boundaries. Cross-diffusion (quasi-soliton) waves have a complex frequency-magnitude relationship and have been classified as a new type of wave (Tsyganov et al., 2007). A particular feature of cross-diffusion waves is that under special circumstances they can lead to extreme events upon collision which are known as rogue waves (Zakharov et al., 2004). A possible scenario for the generation of a catastrophic rogue-wave instability generating earthquakes is described in Regenauer-Lieb et al. (2021).

The relationship between the three types of instabilities is thus argued to be of evolutionary type. A material point should change properties after the propagation of a cross-diffusion excitation wave, and the geological structures formed by either Hopf- or Turing style instabilities are generating internal material interfaces. Therefore, while we predict strictly defined interfaces between the three types of instabilities mathematically, in reality evolutionary crossovers between the instability regimes are expected from excitation waves to Hopf- or Turing instabilities because the material properties evolve dissipatively. Obviously, natural phenomena are restricted in the parameter range, and it is possible that only specific classes of instabilities are encountered due to material coefficients and boundary conditions.

5 Conclusions

In this contribution, we derived a multiphysics and multiscale approach to localisation phenomena in geomaterials by considering explicitly the feedbacks between multiple reaction-diffusion dynamic regimes regularized by considering nonlocal effect of cross-diffusional coupling. This analysis has enriched the classes of stress waves in solids (Kolsky, 1964) by three well defined domains of instability: (1) a narrow domain of Turing instabilities, (2) a broader Hopf domain instability and (3) a new domain of cross-diffusion waves. Both Turing and Hopf instabilities are here proposed to cause geological local-

isation structures of either brittle or ductile nature. We identified diagnostic signatures of these waves, which may be used to test their existence in nature. Turing instabilities have a characteristic wavelength $\lambda = 2\pi/k_c$, Hopf-waves show a characteristic frequency $f = 1/T = \sqrt{\tilde{a}_{11}\tilde{a}_{22} - \tilde{a}_{12}\tilde{a}_{21}}/2\pi$, and cross-diffusional quasisolitons have a characteristic FKPP wave velocity which is a material constant (Tsyganov et al., 2007).

In this work, we substantiated the hypothesis that slow waves propagating as dissipative stress/strain perturbations are a common feature in solids as a result of hierarchically organised multiscale system dynamics (Makarov & Peryshkin, 2017). Seismogenic instabilities themselves are required to couple across the entire range of length scales, from crystal-lattice (chemical) to plate-tectonic scale. This long range multiscale coupling has been proposed by (Regenauer-Lieb et al., 2021) to be facilitated by cross-diffusion waves because of their multiscale frequency spectrum. Future work invites the development of new diagnostic geological and geophysical tools to detect these new types of slow stress waves in solids.

Refer to supplementary material S1.

Movie S1=Turing Instability, S2=Hopf Bifurcation and S3=Quasi-Soliton

References

Adomian, G. (1995). Fisher-kolmogorov equation [Journal Article]. *Applied Mathematics Letters*, *8*(2), 51-52.

Alevizos, S., Poulet, T., Sari, M., Lesueur, M., Regenauer-Lieb, K., & Veveakis, M. (2017). A framework for fracture network formation in overpressurised impermeable shale: Deformability versus diagenesis [Journal Article]. *Rock Mechanics and Rock Engineering*, *50*(3), 689-703.

Amdreo-Valle, F., Mazon, J., Rossi, D., & Toledo-Molero, J. (2010). *Nonlocal diffusion processes* (Vol. 165) [Book]. Providence, Rhode Island: American Mathematical Society. doi: http://dx.doi.org/10.1090/surv/165

Ball, P. (2012). Pattern formation in nature: Physical constraints and self-organising characteristics [Journal Article]. *Architectural Design*, *82*(2), 22-27.

Bouin, E., Henderson, C., & Ryzhik, L. (2017). Super-linear spreading in local and non-local cane toads equations [Journal Article]. *Journal de Mathématiques Pures et Appliquées*, *108*(5), 724-750. Retrieved from `https://www.sciencedirect.com/science/article/pii/S0021782417300636` doi: https://doi.org/10.1016/j.matpur.2017.05.015

Dewers, T., & Ortoleva, P. (1990). Geochemical self-organization iii, a mechanochemical model of metamorphic differentiation [Journal Article]. *American Journal of Science*, *290*(5), 473-521.

Duszek-Perzyna, M., & Perzyna, P. (1996). Adiabatic shear band localization of inelastic single crystals in symmetric double-slip process [Journal Article]. *Archive of Applied Mechanics*, *66*, 369-384.

Eberhard, M., Savojardo, A., Maruta, A., & Römer, R. A. (2017, Oct). Rogue wave generation by inelastic quasi-soliton collisions in optical fibres. *Optics Express*, *25*(23), 28086.

Elphick, K. E., Sloss, C. R., Regenauer-Lieb, K., & Schrank, C. E. (2021). Distribution, microphysical properties, and tectonic controls of deformation

bands in the miocene subduction wedge (whakataki formation) of the hikurangi subduction zone [Journal Article]. *Solid Earth*, *12*(1), 141-170. doi: https://doi.org/10.5194/se-12-141-2021

Fisher, R. A. (1937). The wave of advance of advantageous genes [Journal Article]. *Annals of Eugenics*, *7*(4), 355-369.

Hu, M., Schrank, C., & Regenauer-Lieb, K. (2020). Cross-diffusion waves in hydro-poro-mechanics [Journal Article]. *Journal of the Mechanics and Physics of Solids*.

Kolmogorov, A., Petrovsky, I., & Piskunov, N. (1937). Etude de l'equation de la diffusion avec croissance de la quantite de matiere et son application a un probleme biologique [Journal Article]. *Bulletin Universite de Etat a Moscow*, *1*(1), 1-26.

Kolsky, H. (1964). Stress waves in solids [Journal Article]. *Journal of Sound and Vibration*, *1*(1), 88-110. Retrieved from https://www.sciencedirect.com/science/article/pii/0022460X64900082 doi: https://doi.org/10.1016/0022-460X(64)90008-2

Kuz'min, Y. O. (2012). Deformation autowaves in fault zones [Journal Article]. *Izvestiya, Physics of the Solid Earth*, *48*(1), 1-16. Retrieved from https://doi.org/10.1134/S1069351312010089 doi: 10.1134/S1069351312010089

L'Heureux, I. (2013). Self-organized rhythmic patterns in geochemical systems [Journal Article]. *Philosophical Transactions of the Royal Society A: Mathematical, Physical and Engineering Sciences*, *371*(2004), 20120356.

Lioubashevski, O., Arbell, H., & Fineberg, J. (1996, May). Dissipative solitary states in driven surface waves. *Phys. Rev. Lett.*, *76*, 3959–3962.

Luther, R. (1987). Propagation of chemical reactions in space [Journal Article]. *Journal of Chemical Education*, *64*(9), 740.

Makarov, P. V., & Peryshkin, A. Y. (2017). Slow motions as inelastic strain autowaves in ductile and brittle media [Journal Article]. *Physical Mesomechanics*, *20*(2), 209-221. Retrieved from https://doi.org/10.1134/S1029959917020114 doi: 10.1134/S1029959917020114

Ortoleva, P. J. (1993). Self-organization and nonlinear dynamics in sedimentary basins [Journal Article]. *Philosophical Transactions of the Royal Society of London Series a-Mathematical Physical and Engineering Sciences*, *344*(1670), 171-179. Retrieved from file://D|/pdf/ptrs_1993_344_171.pdf

Ortoleva, P. J. (1994). *Geochemical self-organization* [Book]. New,York: Oxford University Press.

Peacock, D. C. P., Dimmen, V., Rotevatn, A., & Sanderson, D. J. (2017). A broader classification of damage zones [Journal Article]. *Journal of Structural Geology*, *102*, 179-192. Retrieved from https://www.sciencedirect.com/science/article/pii/S019181411730158X doi: https://doi.org/10.1016/j.jsg.2017.08.004

Regenauer-Lieb, K., Hu, M., Schrank, C., Chen, X., Pena Clavijo, S., Kelka, U., ... Jacquey, A. (2021). Cross-diffusion waves as a trigger for multiscale, multi-physics instabilities: Theory [Journal Article]. *Solid Earth*, *12*, 869–883.

Regenauer-Lieb, K., Veveakis, M., Poulet, T., Wellmann, F., Karrech, A., Liu, J., ... Fusseis, F. (2013). Multiscale coupling and multiphysics approaches in earth sciences: Applications [Journal Article]. *Journal of Coupled Systems and Multiscale Dynamics*, *1*(3), 2330-152X/2013/001/042.

Tsyganov, M. A., & Biktashev, V. N. (2014, Dec). Classification of wave regimes in excitable systems with linear cross diffusion. *Phys. Rev. E*, *90*, 062912.

Tsyganov, M. A., Biktashev, V. N., Brindley, J., Holden, A. V., & Genrikh, R. I. (2007). Waves in systems with cross-diffusion as a new class of nonlinear waves [Journal Article]. *Physics-Uspekhi*, *50*(3), 263.

Vanag, V. K., & Epstein, I. R. (2009). Cross-diffusion and pattern formation in reaction–diffusion systems [Journal Article]. *Physical Chemistry Chemical*

534   *Physics*, *11*(6), 897-912.

535   Vardoulakis, I., & Sulem, J.   (1995).   *Bifurcation analysis in geomechanics* [Book].

536   Glasgow: Blankie Acc. and Professional.

537   Vasil'ev, V. A.   (1979).   Autowave processes in distributed kinetic systems [Journal

538   Article]. *Soviet Physics Uspekhi*, *22*(8), 615-639.

539   Veveakis, E., & Regenauer-Lieb, K.   (2015).   Cnoidal waves in solids.   *Journal of the*

540   *Mechanics and Physics of Solids*, *78*, 231-248.

541   Volpert, V., & Petrovskii, S.   (2009).   Reaction–diffusion waves in biology [Journal

542   Article]. *Physics of Life Reviews*, *6*(4), 267-310.

543   Zaiser, M., & Hähner, P. (1997). Oscillatory modes of plastic deformation: Theoreti-

544   cal concepts [Journal Article]. *physica status solidi (b)*, *199*(2), 267-330.

545   Zakharov, V., Dias, F., & Pushkarev, A.   (2004).   One-dimensional wave turbulence

546   [Journal Article]. *Physics Reports*, *398*(1), 1-65.

547   Zuev, L., & Barannikova, S.   (2010).   Plastic flow macrolocalization: Autowave and

548   quasi-particle, [Journal Article].   *Journal of Modern Physics*, *1*(1), 1-8.   doi:

549   https://dx.doi.org/10.4236/jmp.2010.11001
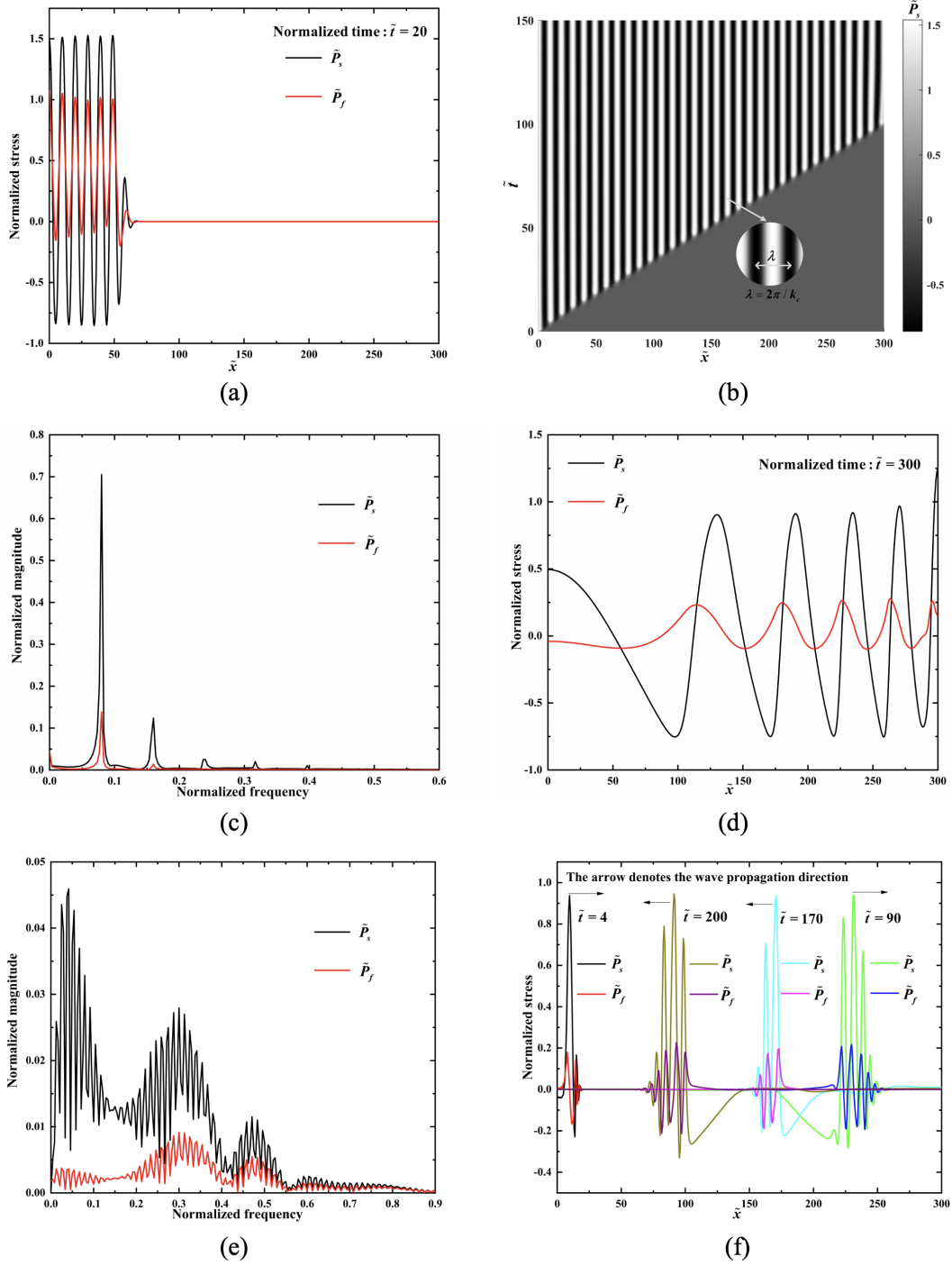
(a)

(b)

(c)

(d)

(e)

(f)

Figure 1. Three types of instabilities. Type-I bifurcation (Turing instability): a) propagating standing wave before reaching the boundary; b) final standing-wave pattern. The dimensionless group of parameters used: $\tilde{a}_{11} = 1.5, \tilde{a}_{12} = -1.3, \tilde{a}_{13} = 1, \tilde{a}_{14} = -1, \tilde{a}_{21} = 2, \tilde{a}_{22} = -1.6, \tilde{D}_M = 1, \tilde{D}_H = 3, \tilde{d}_M = 2, \tilde{d}_H = -1.5$. Type-II (Hopf) bifurcation: c) Hopf waves in frequency domain; d) travelling Hopf waves in space domain. The dimensionless group of parameters used: $\tilde{a}_{11} = 0.3, \tilde{a}_{12} = -3, \tilde{a}_{13} = 0.5, \tilde{a}_{14} = -0.5, \tilde{a}_{21} = 0.1, \tilde{a}_{22} = -0.1, \tilde{D}_M = 0.1, \tilde{D}_H = 0.1, \tilde{d}_M = -1, \tilde{d}_H = 1$. Type-III bifurcation (Quasi-soliton wave): e) Quasi-soliton waves in frequency domain; f) travelling Quasi-soliton waves before and after reflection in space domain. The dimensionless group of parameters used: $\tilde{a}_{11} = -0.05, \tilde{a}_{12} = -3, \tilde{a}_{13} = 1, \tilde{a}_{14} = -1, \tilde{a}_{21} = 0.01, \tilde{a}_{22} = 0, \tilde{D}_M = 0.01, \tilde{D}_H = 0.01, \tilde{d}_M = -1, \tilde{d}_H = 1$.
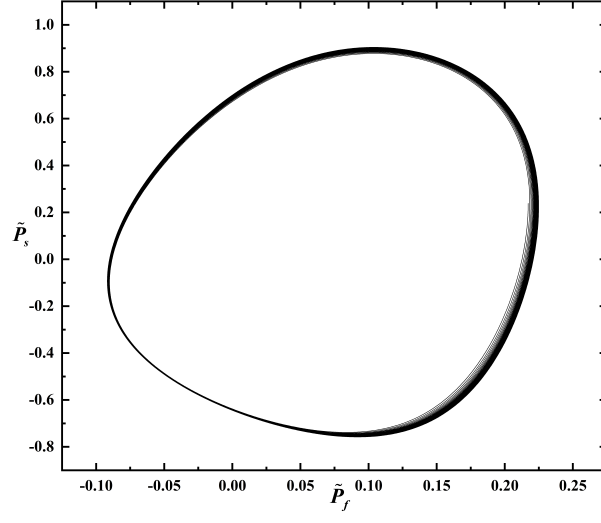
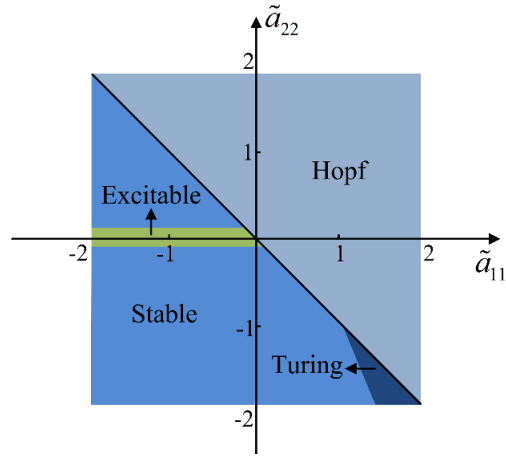**Figure 2.** Phase diagram of Hopf bifurcation upon reaching stable orbits (clockwise oscillation).

Figure 3. Parametric $\tilde{a}_{11}$ versus $\tilde{a}_{22}$ space of instabilities